

Scaffold-assisted synthesis of crystalline mesoporous titania materials

Michał Marszewski and Mietek Jaroniec*

Department of Chemistry and Biochemistry, Kent State University, Kent, OH 44242, USA

Fax: +1 (330) 672-3816; Tel: +1 (330) 672-2032; E-mail: jaroniec@kent.edu

Additional discussion of the materials templated with silica nanoparticles

As-synthesized etched materials from titania and silica nanoparticles. All as-synthesized etched materials have isotherms of type IV with H3 hysteresis loops, according to the IUPAC classification. The as-synthesized etched titania (T-ae) reference sample exhibits type IV isotherm as well, but the hysteresis loop is again small and hard to classify. These features indicate the as-synthesized etched materials are mesoporous with the pores probably created between aggregated nanoparticles. No direct TEM confirmation is available, but the structures of the etched materials should not differ considerably from those of the as-synthesized composites except for the absence of silica nanoparticles due to etching. Moreover, the structure of the T-50Si-ce calcined etched material (Figure 2 panels C and D) shows that the aggregated structures persisted through the calcination and silica etching. Thus, it is safe to assume the as-synthesized etched materials consist of the aggregates of TiO₂ nanoparticles similar to those observed in the as-synthesized composites but with no silica nanoparticles.

The specific surface areas of the as-synthesized etched materials range from 199 to 204 m² g⁻¹ through the series without a clear trend. All values are slightly larger than that of T-ae (192 m² g⁻¹) and slightly smaller compared with those for the respective as-synthesized composites, but it is not possible to make any definitive conclusion due to the relatively large uncertainty of these values. Regardless of the statistical significance, it may be concluded that the loading of silica nanoparticles and their etching had no, or very small, effect on the surface areas of the resulting titania samples. The total pore volume increases from 0.16 to 0.59 cm³ g⁻¹ through the series with increasing amount of the etched scaffold. The values are significantly larger than that of the T-ae titania (0.12 cm³ g⁻¹) by factors of 1.4 (T-10Si-ae), 3.0 (T-30Si-ae), and 5.1 (T-50Si-ae), and compared with the respective as-synthesized composites as well, by factors of 1.2 (T-10Si-ae), 2.2 (T-30Si-ae), and 2.8 (T-50Si-ae). The observed substantial enlargement in the pore volume is attributed to the additional porosity created by removal of silica nanoparticles as in the case for the calcined etched materials (discussed in the main manuscript). Similarly, the experimental pore volumes match the values calculated by assuming a complete removal of silica nanoparticles and preservation of the created voids in the structure (see the calculations below).

The PSD curves of all as-synthesized etched materials exhibit similar shapes, with two distinct broad peaks: the first in the range of small mesopores and the second in the range of large mesopores. In the

former case, the peak's position varies from 2.6 nm to 3.2 nm, increasing slightly through the series, while the peak spans from ca. 1.8 nm to ca. 7 nm. A similarly shaped peak, centered at 2.9 nm and spanning the same range, is present in the PSD curve of the T-ae titania. Consequently, these peaks represent the intra-particle porosity of titania nanoparticles. In the range of large mesopores, the peak's position increases from 20 nm to 28 nm through the series, while the peak spans from roughly 10 nm to almost 60 nm (except the T-50Si-ae material, whose peak spans to almost 90 nm). Similarly to the calcined etched materials (discussed in the main manuscript), this peak appears only for the etched materials and its intensity increases with increasing amount of the etched silica. Moreover, the peak's maximum corresponds well with the size of silica nanoparticles. Thus, this peak reflects the additional porosity created by the removal of silica nanoparticles. In addition, the peak's width varies from the size of a single nanoparticle upwards, indicating some silica nanoparticles are present in the form of aggregates.

Calcined composites of titania and silica nanoparticles. All calcined composites exhibit isotherms of type IV with well-resolved H3 hysteresis loops, according to the IUPAC classification. The reference calcined titania (T-c) has type IV isotherm as well, but the hysteresis loop is small and hard to classify unambiguously. These features indicate that the calcined composites are mesoporous as well, with porosity probably created between aggregated nanoparticles. Although no direct TEM confirmation is available, the composites should not differ considerably from the calcined etched materials (Figure 2 panels C and D), except for the missing silica nanoparticles. Thus, it is safe to assume that the calcined composites consist of the aggregates of TiO₂ nanoparticles similar to those observed in the calcined etched materials, but with the silica nanoparticles still present.

The specific surface areas of the calcined composites increase from 69 to 119 m² g⁻¹ through the series with increasing scaffold amount. The values are smaller compared with those of the corresponding as-synthesized composites by factors of 3.3 (T-10Si-c), 2.1 (T-30Si-c), and 1.7 (T-50Si-c), but are markedly larger than that of the T-c titania (13 m² g⁻¹) by factors of 5.2 (T-10Si-c), 7.5 (T-30Si-c), and 8.9 (T-50Si-c). The total pore volume increases from 0.10 to 0.21 cm³ g⁻¹ through the series as well. In this instance, however, only the T-10Si-c composite shows smaller pore volume (1.3-fold), whereas the T-30Si-c and T-50Si-c composites retained the whole porosity of the as-synthesized composites. In addition, the values are larger than that of the T-c titania (0.02 cm³ g⁻¹) by factors of 4.3 (T-10Si-c), 6.8 (T-30Si-c), and 9.0 (T-50Si-c). The observed reduction in the structural parameters, compared with those of the as-synthesized composites, is a result of titania's crystallization (as discussed for the calcined etched materials in the main manuscript). The composites, however, were much more resistant to this process: while they lost only some of their surface areas and retained almost all pore volume, the reference titania noted over 16-fold surface area reduction

and 6-fold pore volume reduction. Arguably, silica nanoparticles may be a sole or significant contributor to the observed values of the surface area and pore volume ($S_{\text{BET}} = 231 \text{ m}^2 \text{ g}^{-1}$, $V_t = 0.71 \text{ cm}^3 \text{ g}^{-1}$); however, as evidenced by the calcined etched materials (specific surface areas smaller only by 11 % on average after etching), this is not the case.

All calcined composites have similarly shaped PSDs with a single broad peak centered at 8.5 nm (except the T-10Si-c composite, whose peak is centered at lower value, 8.2 nm) spanning from 2.5 nm to 30 nm. A similarly shaped peak, centered at 8.5 nm and spanning from 2.5 to ca. 15 nm is present on the PSD curve of the T-c titania, indicating the lower part of the PSD peak for the composites represents the intra-particle porosity between titania nanoparticles. As discussed for the calcined etched materials (see the main manuscript), titania nanoparticles grew in size due to the calcination-induced crystallization and the same can be concluded for the calcined materials. The upper part of PSD, more pronounced for the composites with higher scaffold content and unaffected by the calcination (silica should not be affected in the temperature range used), is therefore attributed to the intra-particle porosity of silica nanoparticles.

Additional discussion of materials templated with TEOS-generated silica

As-synthesized etched materials from titania and TEOS-generated silica. All as-synthesized etched materials have isotherms of type IV with hysteresis loops of type H3, according to the IUPAC classification, indicating the materials are mesoporous. No TEM images are available, but the etched materials should not differ considerably from the as-synthesized composites (Figure 4 panels A and B), except for the lack of the silica scaffold. In addition, the structure of the T-50Si*-ce calcined etched material (Figure 2 panels C and D) shows that titania nanoparticles stayed aggregated through the calcination and silica etching processes. Thus, it is safe to assume that the as-synthesized etched materials contain aggregates of TiO_2 nanoparticles similar as in the case of the as-synthesized composites but without silica scaffold.

The specific surface areas of the as-synthesized etched materials increase from 222 to 241 $\text{m}^2 \text{ g}^{-1}$ through the series. The values are smaller than those of the respective as-synthesized composites by factors of 1.3 (T-10Si*-ae), 1.6 (T-30Si*-ae), and 1.7 (T-50Si*-ae), but larger (although slightly) compared with that of the T-ae titania (192 $\text{m}^2 \text{ g}^{-1}$) by 16 % (T-10Si*-ae), 23 % (T-30Si*-ae), and 26 % (T-50Si*-ae). The total pore volume increases from 0.18 $\text{cm}^3 \text{ g}^{-1}$ to 0.25 $\text{cm}^3 \text{ g}^{-1}$ through the series as well. Similarly to the surface area, the pore volume is smaller compared with those of the respective as-synthesized composites, 12 % on average, but larger as than that of the T-ae titania (0.12 $\text{cm}^3 \text{ g}^{-1}$) by factors of 1.6 (T-10Si*-ae), 1.9 (T-30Si*-ae), and 2.1 (T-50Si*-ae).

Clearly, the values for the templated titania materials are better (compared with those of the not templated reference titania), showing the TEOS-generated silica benefits the structure of titania. Interestingly, however, it is uncertain if the improvement is due to: 1) the improved structure of titania in the as-synthesized composites or 2) the structure development due to the scaffold removal. For the pore volume, the second option seems more plausible, as the silica removal most certainly creates some new porosity, as in the case of the nanoparticles-templated etched materials. This additional porosity is not as substantial as in the latter case, probably due to the TEOS-generated silica's dispersed nature that would render it less effective in porosity generation. This is supported by the fact that the experimental pore volumes do not match the values calculated by assuming a complete removal of silica and preservation of the emptied space (see calculations below). The first option seems more plausible in the case of surface area enlargement, because the etching could develop new surface area only if silica would be within titania nanoparticles, which is not true in these composites. The PSD curves for all as-synthesized etched materials feature a single broad peak in the range of small mesopores. The peak's position shifts toward larger pore sizes from 3.7 nm to 4.6 nm, through the series with increasing amount of the etched scaffold. The lower bounds are virtually the same at ca. 2 nm; however, the upper bounds shift toward larger values from 10 nm to 14 nm. The PSD curve for the T-ae titania shows a similarly shaped peak, but centered at 2.9 nm and spanning a smaller range of sizes from 1.7 nm to 7 nm. The average and the maximum pore sizes increase are a result of the scaffold removal, indicating that the aggregates of TiO₂ nanoparticles were infiltrated with TEOS-generated silica (as discussed for the calcined etched materials in the main manuscript).

Calcined composites of titania and TEOS-generated silica. All calcined composites have isotherms of type IV with hysteresis loops of type H3 according to the IUPAC classification,³³ indicating that the composites are mesoporous. Although no direct TEM confirmation is available, the TEM images of the T-50Si*-ce calcined etched material (Figure 4 panels C and D) show the TiO₂ nanoparticles retained the aggregated structure through the calcination and silica etching. Thus, it is safe to assume that the calcined composites consist of aggregates of TiO₂ nanoparticles similar as those observed in the calcined etched materials, but embedded in the dough-like TEOS-generated silica as in the case of the as-synthesized composites (Figure 4 panels A and B).

The specific surface areas of the calcined composites increase from 213 to 375 m² g⁻¹ through the series. The values are smaller compared with those of the corresponding as-synthesized composites by factors of 1.3 (T-10Si*-c), 1.2 (T-30Si*-c), and 1.1 (T-50Si*-c), but are markedly larger than that of the T-c titania (13 m² g⁻¹) by factors of 16.3 (T-10Si*-c), 24.5 (T-30Si*-c), and 28.8 (T-50Si*-c). The total pore volume initially increases from 0.20 to 0.25 cm³ g⁻¹ between the T-10Si*-c and the T-30Si*-c composites, and remains constant afterwards. The values are virtually identical

with those of the respective as-synthesized composites (within 10 % uncertainty) and are markedly larger compared with that of the T-c titania ($0.02 \text{ m}^2 \text{ g}^{-1}$) by factors of 10.0 (T-10Si*-c), 12.5 (T-30Si*-c), and 12.5 (T-50Si*-c). Similarly to the nanoparticles-templated calcined composites, the reduction in the surface area is a result of titania's crystallization due to calcination. Importantly, however, these composites are more resistant to this process as well. As previously discussed, the reference titania lost the majority of its surface area and pore volume. The composites, on the other hand, retained the most of the specific surface area and the whole pore volume of the respective as-synthesized composites. Similarly to the other scaffold, the TEOS-generated silica possesses a well-developed structure itself and thus, it may be a significant contributor to the composites' structural parameters. Based on the calcined etched materials—the T-10Si*-ce material retained all surface area of the T-10Si*-c composite, while the values for the T-30Si*-ce and the T-50Si*-ce materials are smaller compared with those of the respective calcined composites by factors of 1.2 and 1.5, respectively—this is true, but the scaffold's presence still improved the titania structures as well. The PSD curves for all calcined composites show only a single peak in the small mesopore range. The peak's position decreases from 4.5 to 2.4 nm through the series, and the peak spans from ca. 2 nm to ca. 13 nm. The PSD curve for the T-c titania shows only a single peak as well that centers at 8.5 nm and spans from ca. 4 nm to ca. 13 nm. Clearly, TiO_2 nanoparticles in the composites have grown much less compared with the T-c ones, but certainly they did grow based on the larger pore sizes than those of the respective as-synthesized composites. It is hard to attribute any specific portion of PSD to the scaffold, which again exemplifies how well the TEOS-generated silica can be integrated with titania nanoparticles.

Calculations

In 1.0 g of the T-30Si-a as-synthesized composite there are: 0.70 g of TiO_2 and 0.30 g of SiO_2 . After etching, the total pore volume will consist of the titania's original porosity and the newly created empty volume after silica removal.

$$\text{TiO}_2 \text{ porosity} = 0.70 \text{ g} \times \text{titania's pore volume} = 0.70 \text{ g} \times 0.12 \text{ cm}^3 \text{ g}^{-1} = 0.084 \text{ cm}^3$$

$$\text{Empty volume} = \text{silica volume} = 0.3 \text{ g} / \text{silica density} = 0.30 \text{ g} / 2.2 \text{ g cm}^{-3} = 0.136 \text{ cm}^3$$

$$\text{Total porosity} = \text{TiO}_2 \text{ porosity} + \text{empty volume} = 0.084 \text{ cm}^3 + 0.136 \text{ cm}^3 = 0.220 \text{ cm}^3$$

$$\text{Total pore volume} = 0.220 \text{ cm}^3 / \text{TiO}_2 \text{ mass} = 0.220 \text{ cm}^3 / 0.70 \text{ g} = 0.314 \text{ cm}^3 \text{ g}^{-1}$$

See table below for a comparison of the calculated values and the experimental pore volumes.

Table S1. Calculated and experimental pore volumes of silica-templated materials.^a

Etched scaffold amount	Calculated V_t ($\text{cm}^3 \text{g}^{-1}$)	Experimental V_t ($\text{cm}^3 \text{g}^{-1}$)			
		T-xSi-ae	T-xSi-ce	T-xSi*-ae	T-xSi*-ce
10 wt%	0.17	<u>0.16</u>	<u>0.15</u>	<u>0.18</u>	<u>0.21</u>
30 wt%	0.31	<u>0.35</u>	<u>0.35</u>	<u>0.22</u>	<u>0.28</u>
50 wt%	0.57	<u>0.59</u>	<u>0.59</u>	<u>0.25</u>	<u>0.31</u>

^a Notation: underline—results repeated for easier comparison; Calculated V_t —total pore volume calculated assuming a complete removal of silica and preservation of the emptied volume and considering TiO_2 porosity of $0.12 \text{ cm}^3 \text{g}^{-1}$; Experimental V_t —total pore volume calculated by conversion of nitrogen adsorbed at a relative pressure of ~ 0.99 to the volume of liquid nitrogen at the experiment conditions, i.e., assuming a density conversion factor of 0.0015468

Table S2. Crystalline properties of the silica-templated materials.^a

Sample	Phase ^b	Anatase crystal size (nm)	Rutile crystal size (nm)	Sample	Phase	Anatase crystal size (nm)	Rutile crystal size (nm)
T-ce	A/R	31.0	48.1	<u>T-ce</u>	<u>A/R</u>	<u>31.0</u>	<u>48.1</u>
T-10Si-ce	A/R	16.0	38.6	T-10Si*-ce	A	5.7	—
T-30Si-ce	A/R	13.0	22.3	T-30Si*-ce	A	5.0	—
T-50Si-ce	A/R	10–11 ^c	10–12 ^c	T-50Si*-ce	A	4.8	—
T-30Si-a	A	4.7	—				
T-30Si-c	A/R	12.5	16 ^c				
<u>T-30Si-ce</u>	<u>A/R</u>	<u>13.0</u>	<u>22.3</u>				

^a Notation: underline—results repeated for easier comparison; symbols with a, ae, c, and ce refer to the as-synthesized, as-synthesized etched, calcined, and calcined etched samples respectively; silica scaffold was delivered in form of either silica nanoparticles (symbols without *) or generated through hydrolysis and condensation of tetraethyl orthosilicate (symbols with *); A denotes anatase phase (matched to ICDD PDF# 00–021–1272); R denotes rutile phase (matched to ICDD PDF# 00–021–1276); crystal size was calculated based on the X-ray diffraction data using Scherrer equation with full width at half-maximum of the most intense peak for the respective phase corrected for the instrumental peak broadening; ^b except T-ce, all samples showed only minute amounts of rutile; ^c the result carries high uncertainty due to inconsistent fitting.

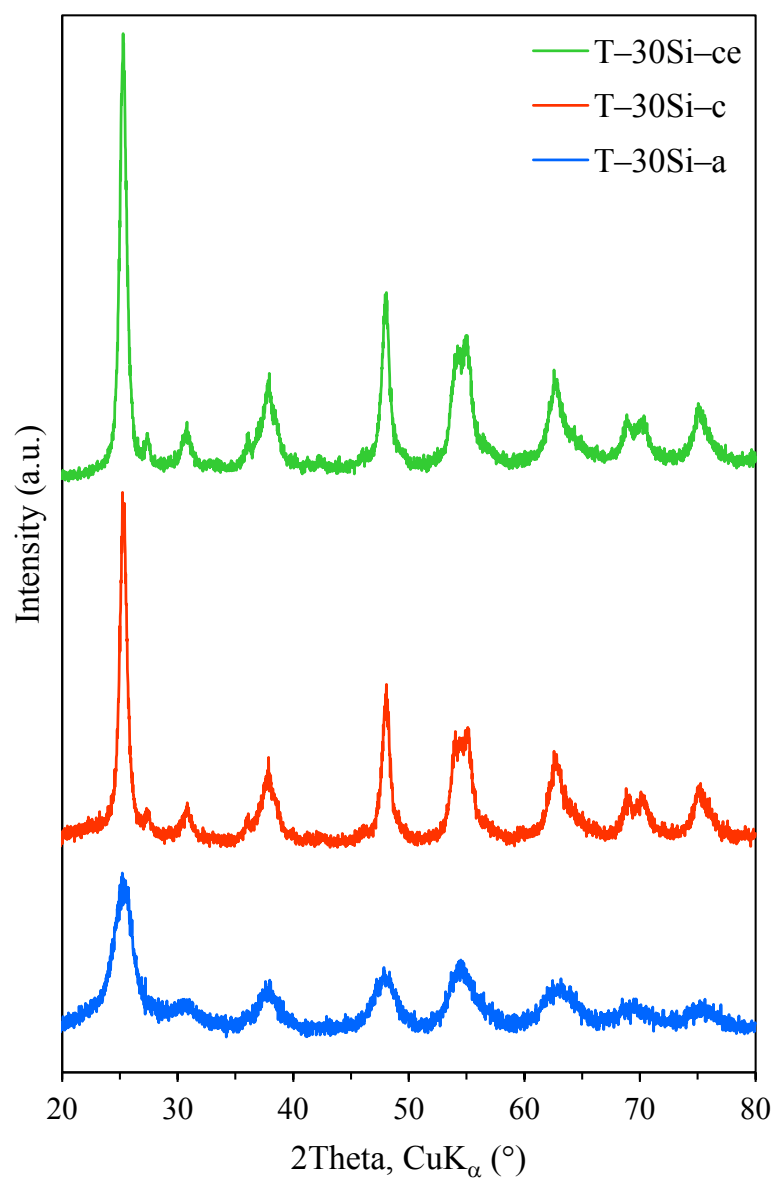


Figure S1. XRD patterns of the as-synthesized, calcined, and calcined etched materials prepared with 30 wt% of silica nanoparticles. T-30Si-a denotes as-synthesized composite prepared with 30 wt% of silica nanoparticles; T-30Si-c denotes calcined composite prepared with 30 wt% of silica nanoparticles; T-30Si-ce denotes calcined etched titania prepared with 30 wt% of silica nanoparticles.

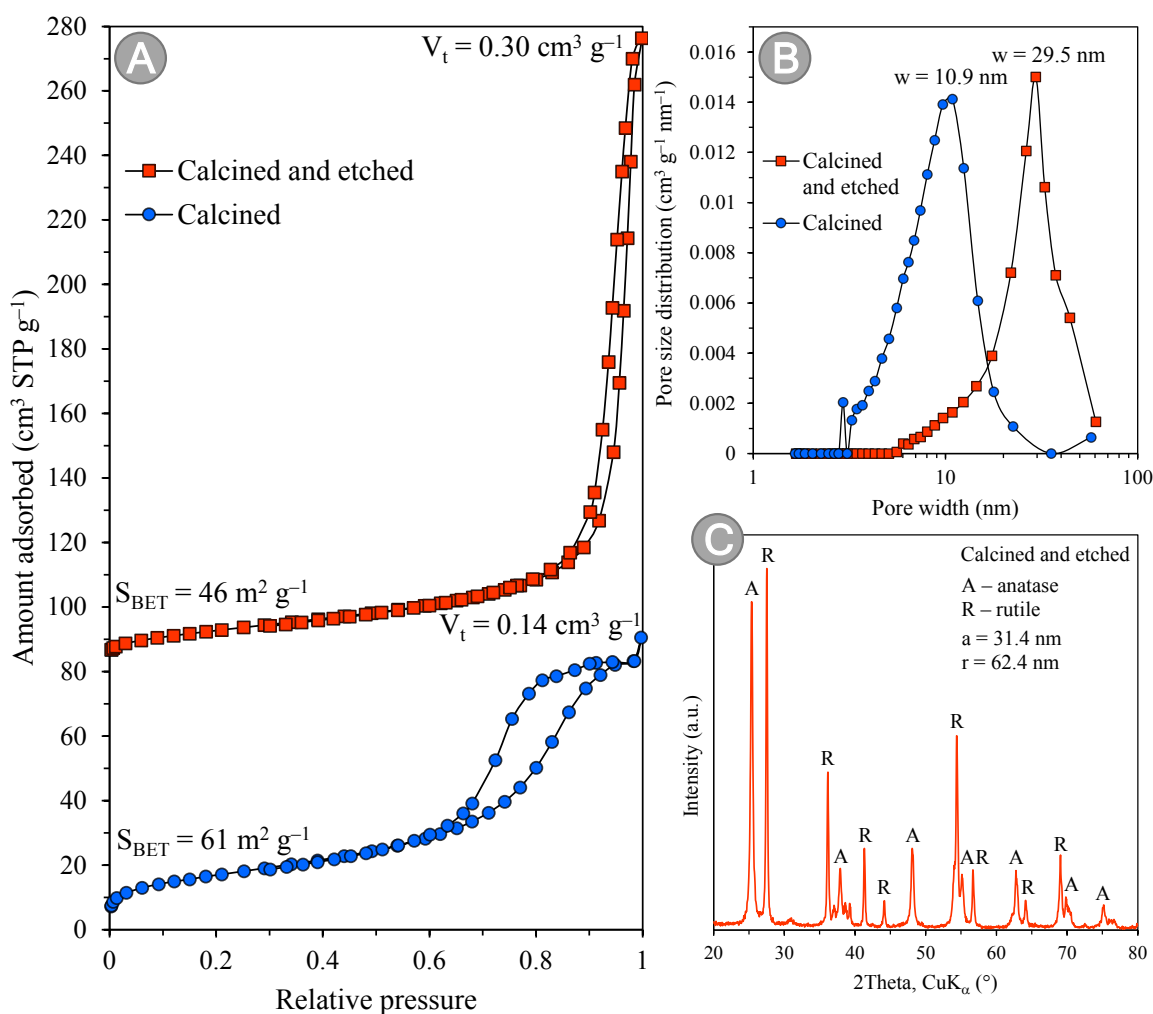


Figure S2. Characterization of the titania samples templated with 30 wt% of silica nanoparticles after calcination at 800 °C and after calcination and NaOH etching: (A) nitrogen adsorption–desorption isotherms measured at –196 °C, and the BET specific surface areas (S_{BET}) and total pore volumes (V_t) values shown close to the corresponding isotherms (the isotherm for the calcined etched material shifted up by 80 cm³ STP g⁻¹); (B) pore size distribution calculated based on the nitrogen adsorption data and the pore sizes (w) indicated close to the corresponding peaks maxima; and (C) XRD patterns of the calcined etched material, and the anatase (a) and rutile (r) crystal sizes; letter A indicates peaks matching the anatase phase (ICDD PDF# 00–021–1272); letter R indicates peaks matching the rutile phase (ICDD PDF# 00–021–1276).

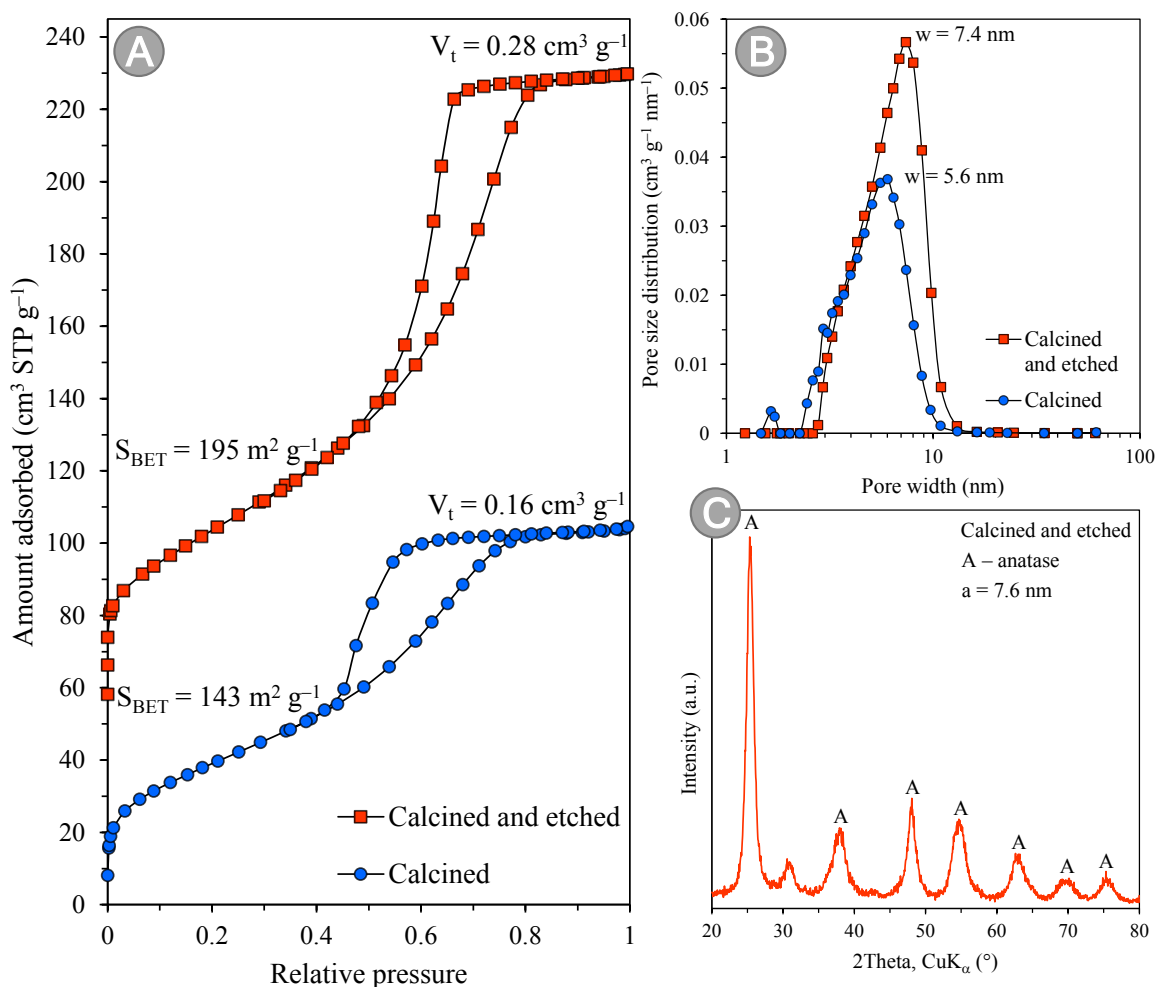


Figure S3. Characterization of the titania samples templated with 30 wt% of TEOS-generated silica after calcination at 800 °C and after calcination and NaOH etching: (A) nitrogen adsorption–desorption isotherms measured at $-196 \text{ }^\circ\text{C}$, and the BET specific surface areas (S_{BET}) and total pore volumes (V_t) shown close to the corresponding isotherms (the isotherm for the calcined etched material shifted up by $50 \text{ cm}^3 \text{ STP g}^{-1}$); (B) pore size distribution calculated based on the nitrogen adsorption data and the pore sizes (w) indicated close to the corresponding peaks maxima; and (C) XRD patterns of the calcined etched material, and the anatase (a) crystal size; letter A indicates peaks matching the anatase phase (ICDD PDF# 00–021–1272).

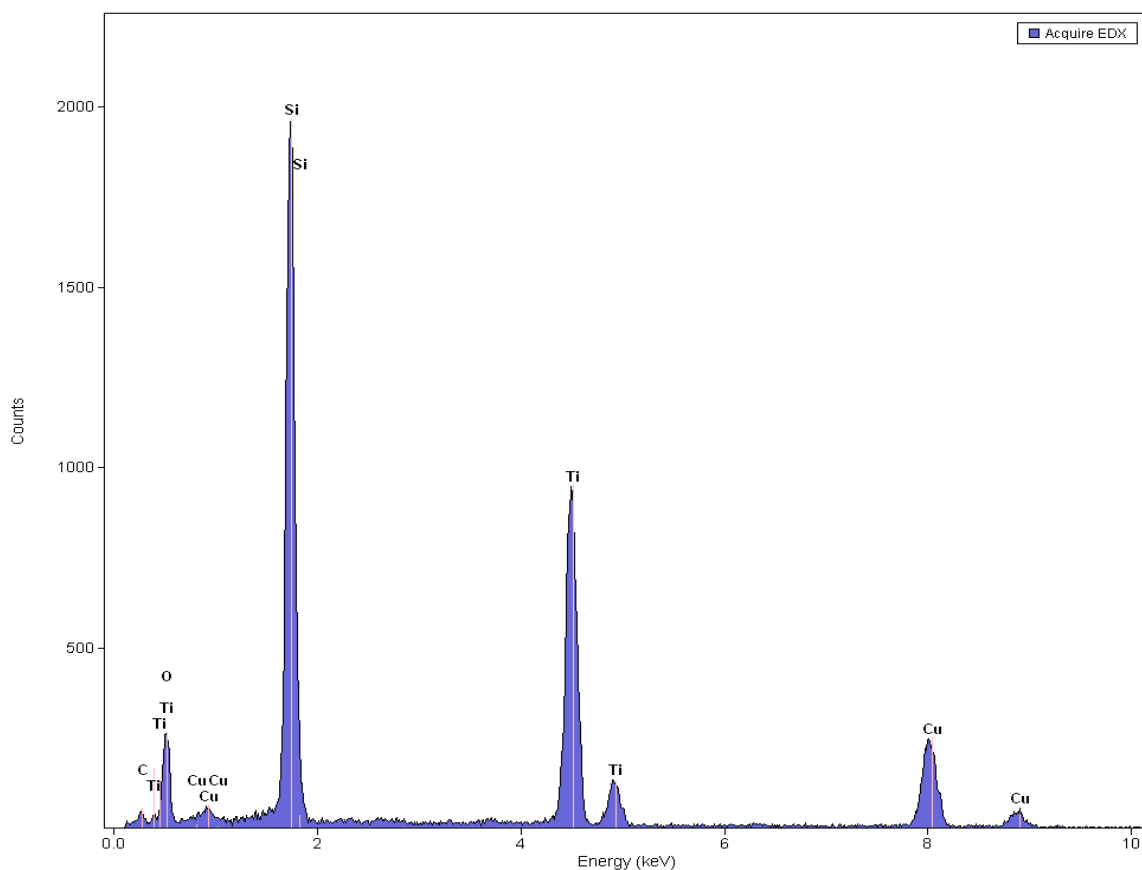


Figure S4. Energy-dispersive X-ray (EDX) spectrum of T-30Si-c (the calcined composite prepared with 50 wt% of silica nanoparticles).

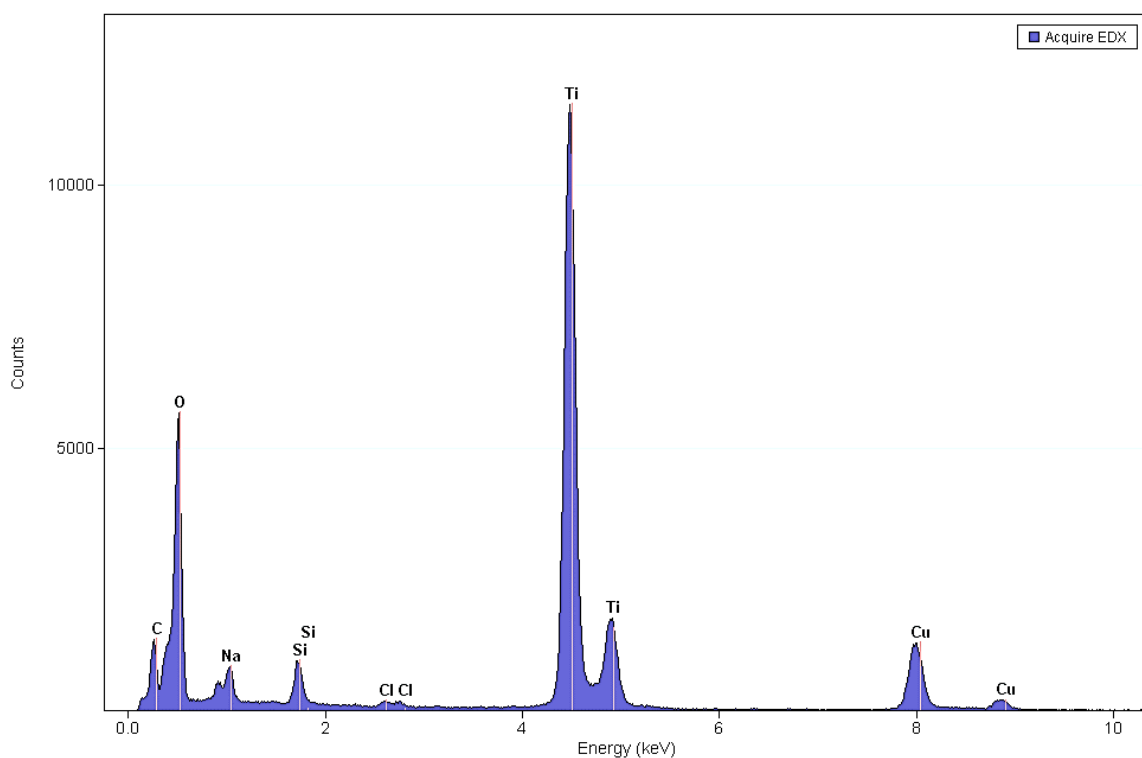


Figure S5. Energy-dispersive X-ray (EDX) spectrum of T-50Si-ce (the calcined etched titania prepared with 50 wt% of silica nanoparticles).

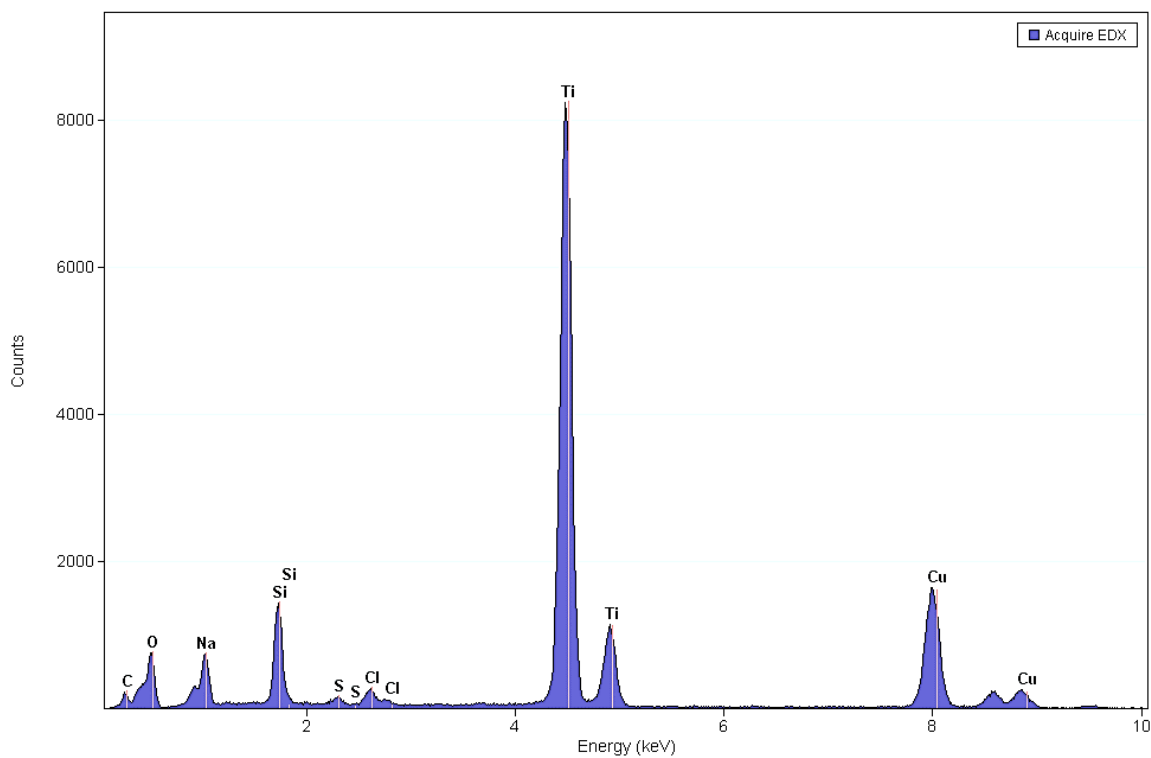


Figure S6. Energy-dispersive X-ray (EDX) spectrum of T-50Si*-ce (the calcined etched titania prepared with 50 wt% of TEOS-generated silica; TEOS denotes tetraethyl orthosilicate).

Table S3. Structural parameters of alumina-templated materials.^a

Sample name	S_{BET} ($\text{m}^2 \text{g}^{-1}$)	V_{t} ($\text{cm}^3 \text{g}^{-1}$)	w (nm)	Sample name	S_{BET} ($\text{m}^2 \text{g}^{-1}$)	V_{t} ($\text{cm}^3 \text{g}^{-1}$)	w (nm)
<u>T-a</u>	<u>211</u>	<u>0.12</u>	<u>2.7</u>	<u>T-a</u>	<u>211</u>	<u>0.12</u>	<u>2.7</u>
T-10Al-a	231	0.13	2.7	T-10Al*-a	238	0.14	2.8
T-30Al-a	274	0.16	2.9	T-30Al*-a	203	0.13	2.6
T-50Al-a	299	0.19	3.2	T-50Al*-a	213	0.14	3.1
<u>T-ae</u>	<u>192</u>	<u>0.12</u>	<u>2.9</u>	<u>T-ae</u>	<u>192</u>	<u>0.12</u>	<u>2.9</u>
T-10Al-ae	183	0.14	2.8	T-10Al*-ae	242	0.15	3.1
T-30Al-ae	221	0.24	3.2	T-30Al*-ae	263	0.26	3.4
T-50Al-ae	232	0.30	3.5	T-50Al*-ae	269	0.27	4.2
<u>T-c</u>	<u>13</u>	<u>0.02</u>	<u>8.5</u>	<u>T-c</u>	<u>13</u>	<u>0.02</u>	<u>8.5</u>
T-10Al-c	117	0.12	5.3	T-10Al*-c	132	0.15	5.8
T-30Al-c	177	0.19	5.1	T-30Al*-c	180	0.15	4.0
T-50Al-c	228	0.24	5.0	T-50Al*-c	213	0.18	4.0
<u>T-ce</u>	<u>15</u>	<u>0.04</u>	<u>7.8</u>	<u>T-ce</u>	<u>15</u>	<u>0.04</u>	<u>7.8</u>
T-10Al-ce	112	0.15	5.9	T-10Al*-ce	143	0.15	5.6
T-30Al-ce	152	0.27	6.7	T-30Al*-ce	187	0.16	4.0
T-50Al-ce	195	0.44	7.2	T-50Al*-ce	220	0.22	4.7
Catpal A	314	0.35	4.6				

^a Notation: underline—results repeated for easier comparison; symbols with a, ae, c, and ce refer to the as-synthesized, as-synthesized etched, calcined, and calcined etched samples respectively; alumina scaffold was delivered in form of either boehmite nanoparticles (symbols without *) or generated through hydrolysis and condensation of aluminium isopropoxide (symbols with *). S_{BET} —specific surface area calculated using the Brunauer–Emmett–Teller (BET) method in a relative pressure range 0.05–0.20, assuming a nitrogen cross-section area of 0.162 nm²; V_{t} —total pore volume calculated by conversion of nitrogen adsorbed at a relative pressure of ~0.99 to the volume of liquid nitrogen at the experiment conditions, i.e. assuming a density conversion factor of 0.0015468; w—pore size estimated as the center or maximum of the peak on the pore size distribution calculated using the Kruk–Jaroniec–Sayari (KJS) method based on the low-temperature nitrogen adsorption data and using a modified Kelvin equation for cylindrical mesopores, and an experimental statistical film thickness curve measured on a reference macroporous silica LiChrospher Si-1000

Table S4. Crystalline properties of the alumina-templated materials.^a

Sample name	Phase	Anatase crystal size (nm)	Rutile crystal size (nm)	Sample name	Phase	Anatase crystal size (nm)	Rutile crystal size (nm)
<u>T-ce</u>	<u>A/R</u>	<u>31.0</u>	<u>48.1</u>	<u>T-ce</u>	<u>A/R</u>	<u>31.0</u>	<u>48.1</u>
T-10Al-ce	A	8.5	—	T-10Al*-ce	A	6.2	—
T-30Al-ce	A	6.7	—	T-30Al*-ce	A	5.2	—
T-50Al-ce	A	5.9	—	T-50Al*-ce	A	5.0	—
T-30Al-a	A	4.6	—				
T-30Al-c	A	6.5	—				
<u>T-30Al-ce</u>	<u>A</u>	<u>6.7</u>	—				

^a Notation: underline—results repeated for easier comparison; symbols with a, ae, c, and ce refer to the as-synthesized, as-synthesized etched, calcined, and calcined etched samples respectively; alumina scaffold was delivered in form of either boehmite nanoparticles (symbols without *) or generated through hydrolysis and condensation of aluminium isopropoxide (symbols with *); A denotes anatase phase (matched to ICDD PDF# 00-021-1272); R denotes rutile phase (matched to ICDD PDF# 00-021-1276); crystal size was calculated based on X-ray diffraction data using Scherrer equation with full width at half-maximum of the most intense peak for the respective phase corrected for the instrumental peak broadening.

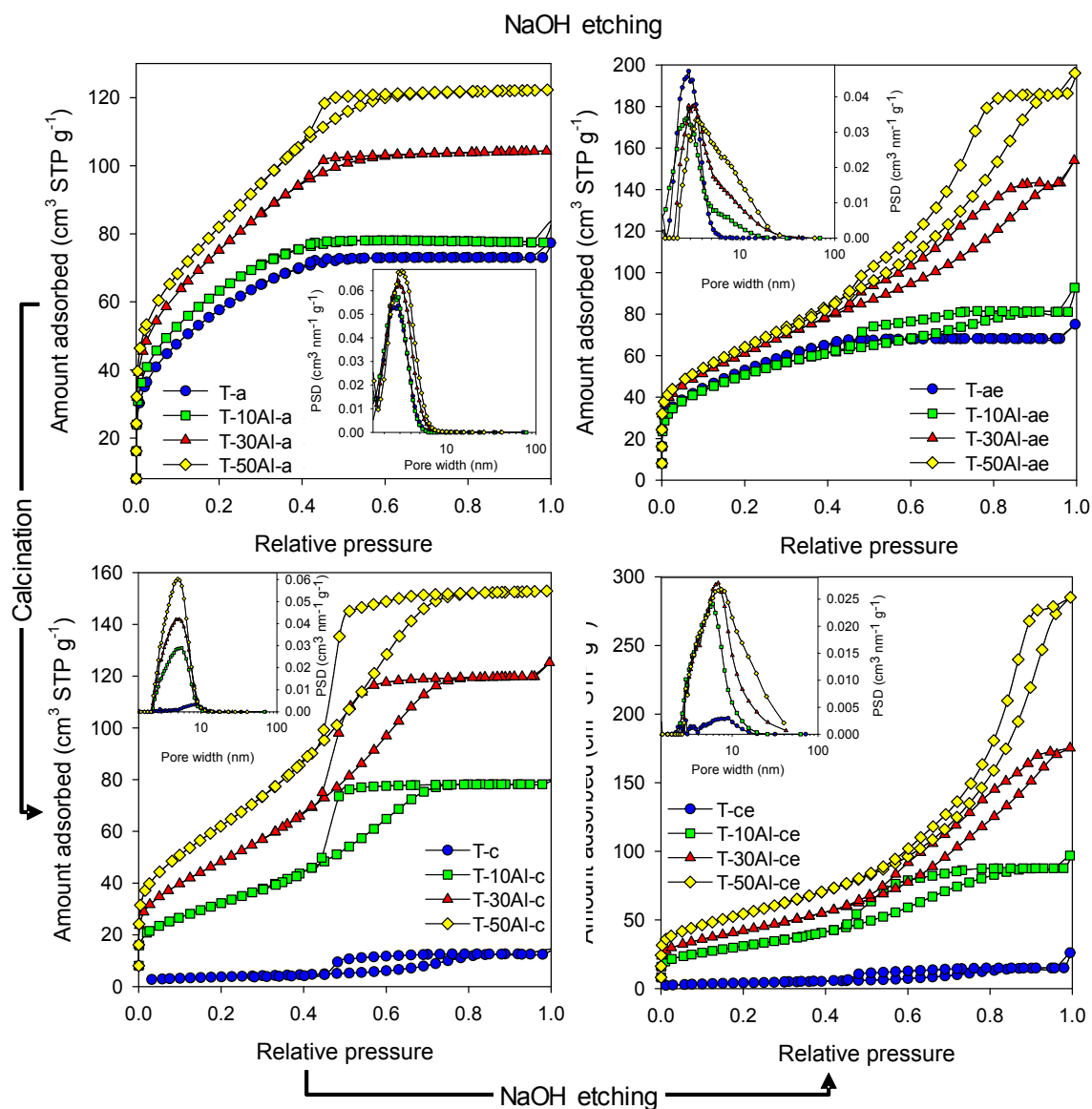


Figure S7. Nitrogen adsorption–desorption isotherms measured at $-196\text{ }^{\circ}\text{C}$ and the corresponding pore size distributions (PSD; insets) measured for titania materials templated with 10, 30, and 50 wt% of alumina particles: as–synthesized (top left), as–synthesized etched (top right), calcined (bottom left), and calcined etched (bottom right). Adsorption isotherms and PSD curves for the corresponding titania materials, prepared without addition of silica nanoparticles: T–a, T–ae, T–c, and T–ce are also shown for the purpose of comparison.

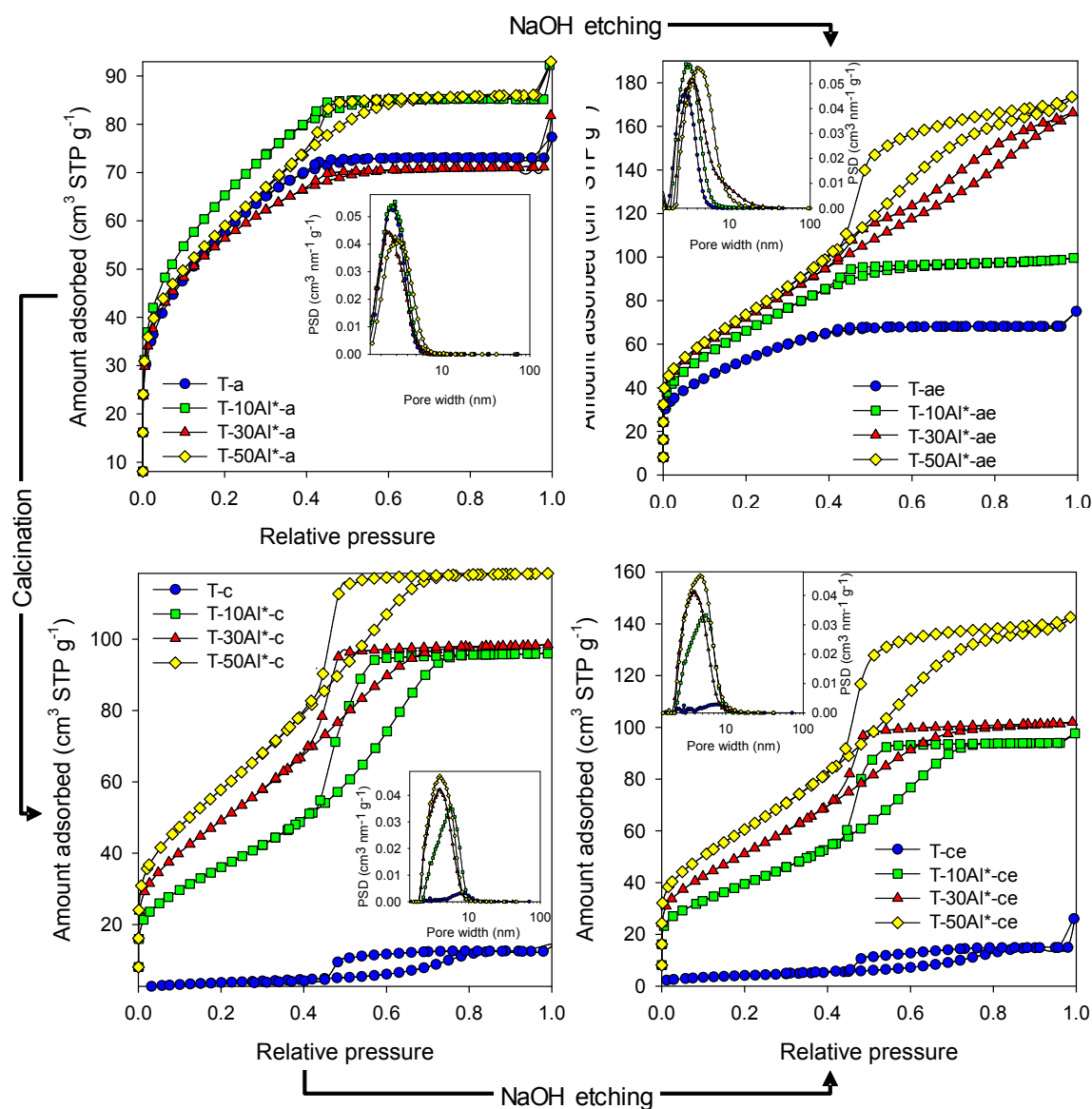


Figure S8. Nitrogen adsorption–desorption isotherms measured at $-196\text{ }^{\circ}\text{C}$ and the corresponding pore size distributions (PSD; insets) measured for titania materials templated with 10, 30, and 50 wt% of AIPO-generated–alumina: as–synthesized (top left), as–synthesized etched (top right), calcined (bottom left), and calcined etched (bottom right). Adsorption isotherms and PSD curves for the corresponding titania materials, prepared without addition of silica nanoparticles: T–a, T–ae, T–c, and T–ce are also shown for the purpose of comparison.

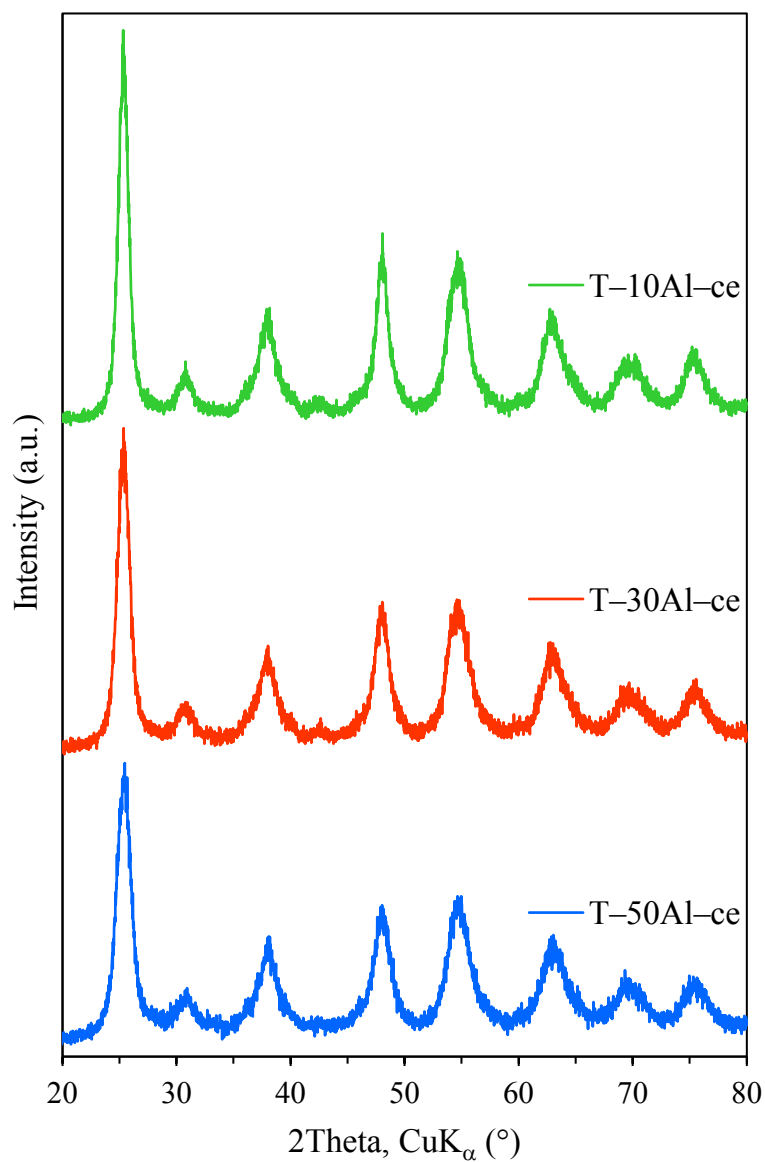


Figure S9. XRD patterns of the calcined etched titania samples prepared with 10, 30, and 50 wt% of boehmite alumina particles. T-10Al-ce denotes calcined etched titania prepared with 10 wt% of boehmite alumina particles; T-30Al-ce denotes calcined etched titania prepared with 30 wt% of boehmite alumina particles; T-50Al-ce denotes calcined etched titania prepared with 50 wt% of boehmite alumina particles.

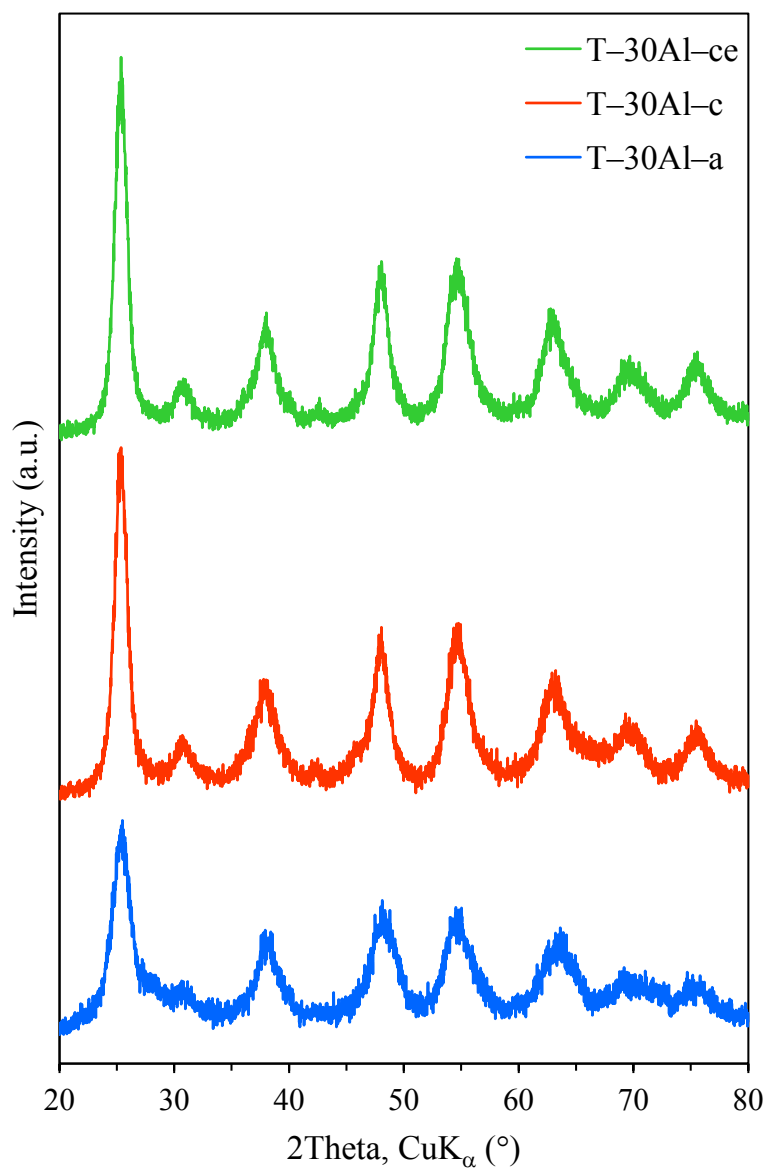


Figure S10. XRD patterns of the as-synthesized, calcined, and calcined etched materials prepared with 30 wt% of boehmite alumina particles. T-30Al-a denotes as-synthesized composite prepared with 30 wt% of boehmite alumina particles; T-30Al-c denotes calcined composite prepared with 30 wt% of boehmite alumina particles; T-30Al-ce denotes calcined etched titania prepared with 30 wt% of boehmite alumina particles.

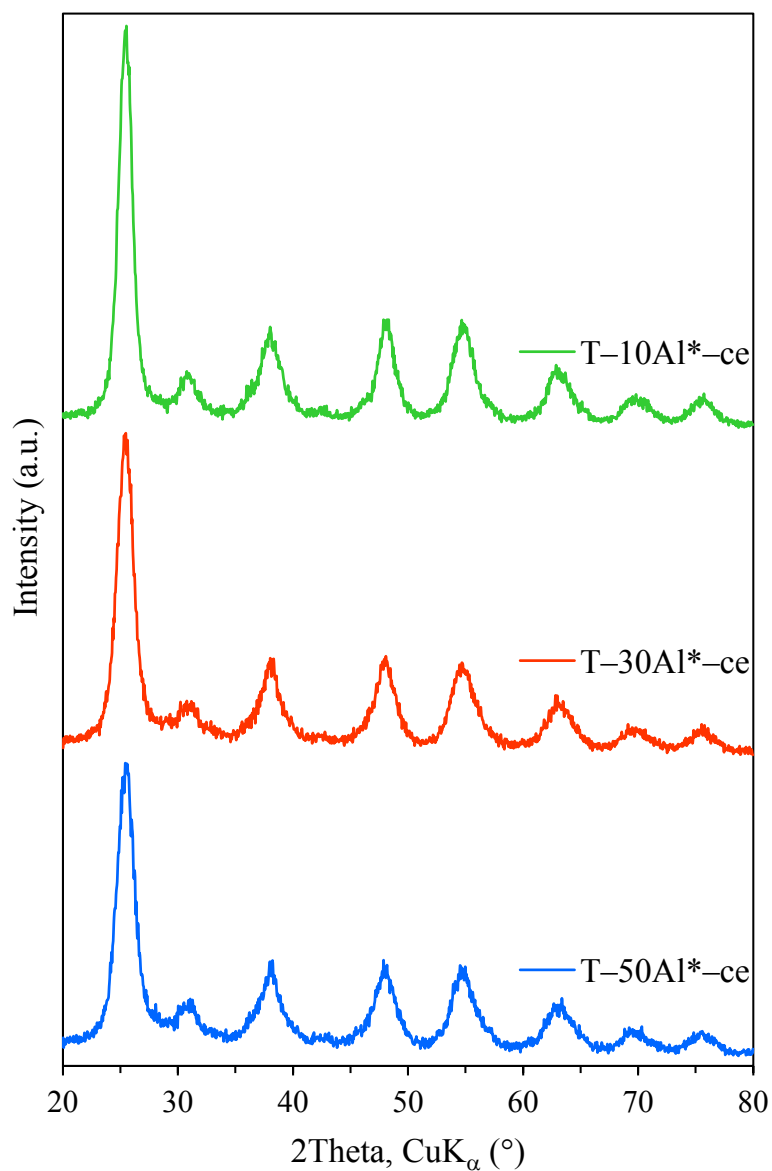


Figure S11. XRD patterns of the calcined etched titania samples prepared with 10, 30, and 50 wt% of AIPO-generated alumina. AIPO denotes aluminium isopropoxide; T-10Al*-ce denotes calcined etched titania prepared with 10 wt% of AIPO-generated alumina; T-30Al-ce denotes calcined etched titania prepared with 30 wt% of AIPO-generated alumina; T-50Al-ce denotes calcined etched titania prepared with 50 wt% of AIPO-generated alumina.

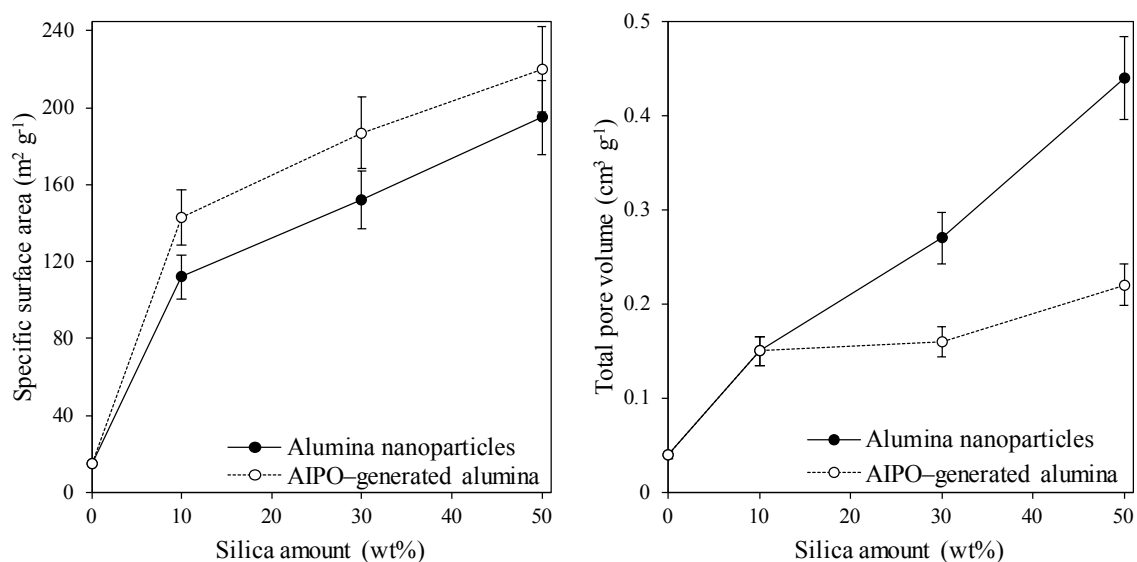


Figure S12. Comparison of structural parameters: specific surface area (left) and total pore volume (right) for the calcined etched titania materials templated with either alumina nanoparticles or AIPO-generated alumina. Connecting lines serve as guides only; AIPO denotes aluminum isopropoxide; error bars represent 10 % uncertainty.

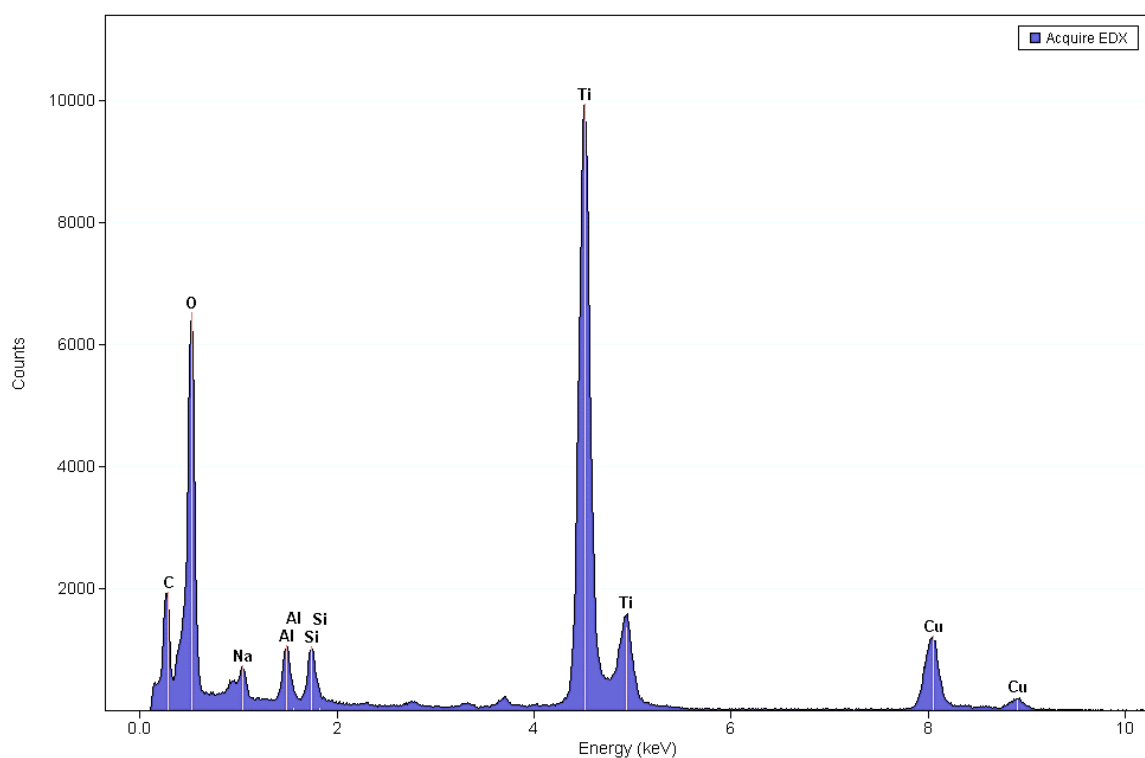


Figure S13. Energy-dispersive X-ray (EDX) spectrum of T-50Al-ce (the calcined etched titania prepared with 50 wt% of boehmite alumina particles).

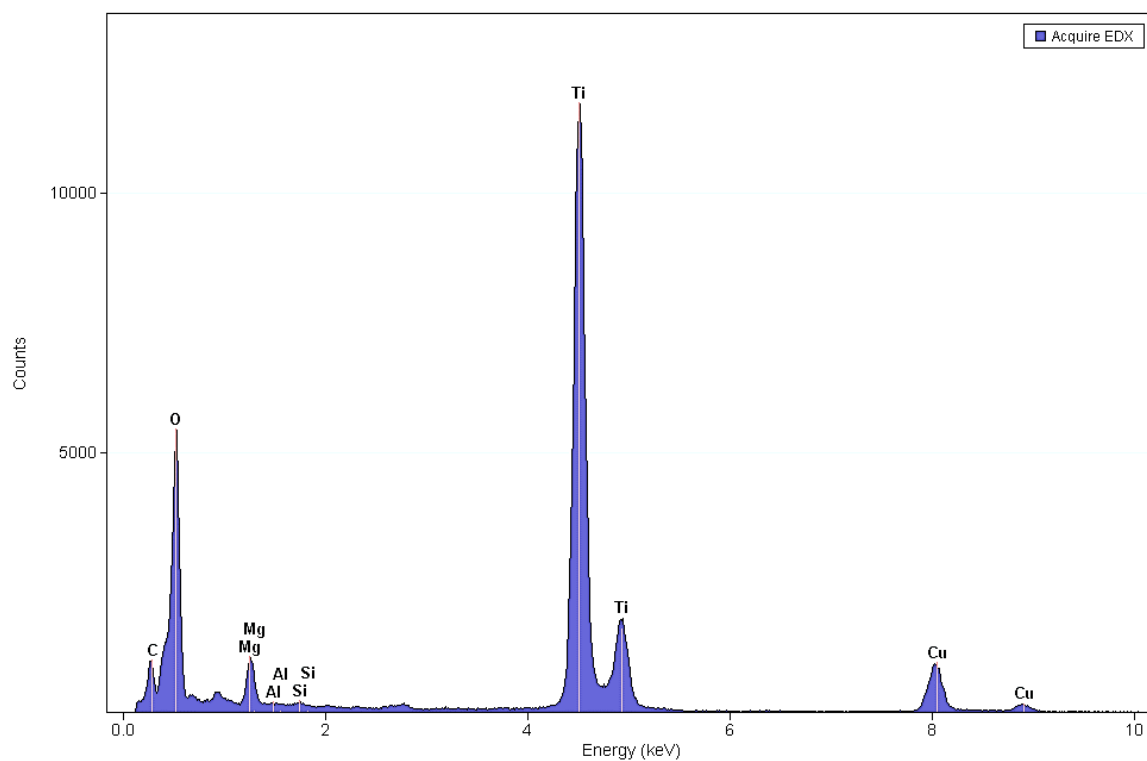


Figure S14. Energy-dispersive X-ray (EDX) spectrum of T-50Al*-ce (the calcined etched titania prepared with 50 wt% of AIPO-generated alumina; AIPO denotes aluminium isopropoxide).